Temperature inversions in France – Part A: time variations

Daniel Joly, Yves Richard

Climatologie 2022, 19, 4

https://doi.org/10.1051/climat/202219004

Available online :
https://climatology.edpsciences.org

Temperature inversions in France – Part A: time variations

Daniel Joly [1*], Yves Richard [2]

[1] Laboratoire ThéMA, CNRS and Université Bourgogne Franche-Comté, Besançon, France

[2] Centre de Recherches de Climatologie / Biogéosciences, CNRS and Université Bourgogne Franche-Comté, Dijon, France

Résumé – Inversions de température en France – Partie A : variations temporelles. Les inversions de température en France métropolitaine sont calculées au moyen d'un réseau de 859 sites d'échantillonnage répartis sur le territoire. Chaque site comprend deux stations situées à moins de 30 km l'une de l'autre. Nous utilisons les températures quotidiennes minimales (tn) et maximales (tx) des stations météorologiques de Météo-France sur 10 ans. Les variations temporelles de trois caractéristiques d'inversion (fréquence, intensité et durée) sont explorées. Le premier résultat est la fréquence élevée des inversions. En moyenne, pour les 859 sites, les inversions tn se produisent sur 63 % des jours et les inversions tx sur 22,6 %. L'intensité des inversions est généralement faible, le mode étant de 2°C (tn) et 1°C (tx). Cependant, des intensités élevées peuvent être atteintes (maximum 23,6°C pour tn et 22,6°C pour tx). La plus longue séquence d'inversions tn isolées (l'inversion est détruite dans la journée mais se reproduit sur plusieurs jours) a duré plus de 4 mois (126 jours). Ces inversions se produisent le plus souvent d'août à octobre. La plus longue séquence d'inversions tx isolées (l'inversion est détruite pendant la nuit) a duré 38 jours. De telles inversions sont les plus fréquentes de novembre à février. Les inversions persistantes (nuit et jour) sont les plus fréquentes de novembre à janvier ; la plus longue a duré 88 jours. L'ensemble des résultats révèle un certain nombre de points originaux : l'existence d'un grand nombre de séquences d'inversion tx, le schéma saisonnier différenciant très nettement les inversions tn et tx, et l'influence des conditions atmosphériques, notamment la nébulosité.

Mots-clés : inversion de température, intensité, fréquence, durée, variation mensuelle, gradient thermique altitudinal, conditions atmosphériques.

Abstract – Temperature inversions in mainland France are computed using a network of 859 sampling sites spread as evenly as possible across the country. Each site comprises a high station located within 30 km of the low station with which it is paired. We use the daily minimum (tn) and maximum (tx) temperatures from Météo-France weather stations over 10 years (2008–2017). The time variations of three inversion characteristics (frequency, intensity, and duration) are explored. The primary result is the high frequency of inversions. On average, for the 859 sites, tn-inversions occur on 63% of days and tx-inversions on 22.6%. Inversion intensity is usually weak, the mode being 2°C for tn and 1°C for tx. However, high intensities may be reached (maximum 23.6°C for tn and 22.6°C for tx). The longest sequence of isolated tn-inversions (the inversion is destroyed in the daytime but recurs over several days) ran for more than four months (126 days). Such inversions occur most frequently from August to October. The longest sequence of isolated tx-inversions (the inversion is destroyed overnight) ran for 38 days. Such inversions are most common from November to February. The longest persistent inversion (night and day) lasted 88 days. Persistent inversions occur most frequently from November to January. The results as a whole reveal a number of original points: the existence of a large number of tx-inversion sequences, the seasonal pattern very clearly differentiating tn- and tx-inversions, and the significance of atmospheric conditions.

Keywords: temperature inversion, intensity, frequency, duration, monthly variation, altitudinal temperature lapse rate, weather conditions.

* Auteur de correspondance : daniel.joly@univ-fcomte.fr

Introduction

The number of studies of temperature inversions has increased in recent decades owing to growing interest in pollution problems (El Melki, 2007; Chemel *et al.*, 2016; Largeron and Staquet, 2016a, 2016b; Czarnecka and Nidzgorska-Lencewicz, 2017). While commonplace, this phenomenon induces specific ecological conditions and locally generates biotopes (Schlaghamersky *et al.*, 2014) or agricultural conditions (Paraschiv, 2010) that contrast with adjacent areas. Accordingly, thorough knowledge of the inversions that develop in the lower layers of the atmosphere makes for better management of natural and agricultural resources (Fritz *et al.*, 2008; Bish *et al.*, 2019).

Several types of thermal inversions can be observed. In mid-latitudes, the commonest inversions are radiative. The intensity and extent of such inversions vary with atmospheric and topographic conditions. Temperatures fall especially at night when there is a shortfall in solar radiation and when the net radiation at the ground surface becomes negative (Sheridan *et al.*, 2014). Conditions conducive to such a phenomenon prevail especially at ground level when the weather is dry, with little cloud cover and no wind, which is often associated with high-pressure conditions (Barry, 2008; Vosper and Brown, 2008; Vosper *et al.*, 2014; Conangla *et al.*, 2018) and when the cold air layer that develops is partly decoupled from the synoptic flow (Lundquist *et al.*, 2008; Daly *et al.*, 2010; Dorninger et al., 2011). Such inversions are often faint, especially when the cold-air pool is thin. The high winds associated with the passage of a weather system may then temporarily and partially disperse the cold air (Lareau and Horel, 2015a, 2015b). In most cases these inversions are destroyed in the early morning hours by convective turbulence (Anquetin *et al.*, 1998), but, if weather conditions and the topographical context allow, they may last several days (Vitasse, 2017; Sheridan, 2019). Conversely, disturbed weather with cloud and wind is not conducive to the formation of inversions (Williams and Thorp, 2015). There is another type of inversion that is quite frequent at temperate latitudes. This is the subsidence inversion that occurs under warm, high-pressure conditions at high altitudes by adiabatic air compression (Joly and Richard, 2019; Arduini *et al.*, 2020). Subsidence inversions affect large areas and are responsible for the cloud seas that cover plains and valleys while only mountain summits remain clear. Radiative inversion and subsidence phenomena are reinforced by local topography (Anquetin *et al.*, 1998; Fallot, 2012). Whatever the type of inversion, cold air, because it is denser than warmer air, migrates down slopes and accumulates at the bottom of depressions (Helmis and Papadopoulos, 1996; Mahrt *et al.*, 2010; Fernando *et al.*, 2013; Burns and Chemel, 2015). In deep valleys in mountain areas for example, cold air may build up into a column exceeding 1000 m and persist for long periods of time (Largeron and Staquet, 2016b).

Most studies of heat inversions relate to a single mountain range or even to just a part of a range (Li *et al.*, 2012; Wang *et al.*, 2015; Vitasse *et al.*, 2017). This is how we set about our previous studies of the Jura Mountains in France (Joly *et al.*, 2019a, 2019b) where our work on inversion characteristics was carried out using measurements collected from 16 sites located under forest cover. Few studies encompass large areas (Bailey *et al.*, 2011). Considering just a single mountain range or a small area presupposes that inversions are preferentially meso-scale phenomena. It can be assumed that inversions seldom occur over large areas because the associated synoptic conditions would not be uniform enough for inversions to form synchronously and endure over a huge region comprising several separate mountain ranges. And yet, although they are not synchronous, do inversions that develop in and around several mountain ranges share common features? The method developed for the Jura Mountains of France (Joly and Richard, 2018, 2019) can be fully transposed to other regions. This method rests on developing and analysing indices built around temperature data recorded in situ by Météo-France. It can be generalized to all times of the year and to all areas, whether mountainous or not.

The objective of this work is to identify three characteristics of inversions (intensity, frequency, and duration) and their variations over time. This analysis, based on a large documentary database, is essential to the understanding of a phenomenon that is often studied in small areas. After presenting the

area of study, continental France, the first section of this work sets out the data and the method. In the results section, variations of these three characteristics are analysed separately and then synthetically via an ascending hierarchical classification. The discussion section examines the criteria used for defining inversions in this paper. Lastly, inversion characteristics are analysed with respect to weather conditions summarized by daily temperature amplitudes.

1. Data and method

The study area, mainland France (551 000 km²), is a climatically heterogeneous area with a Mediterranean climate in the south, an oceanic climate in the west and continental tendencies in the east, along with marked mountain characteristics with elevation (Joly *et al.*, 2010). This climatic pattern is related to latitude and to France having three coastlines, with the English Channel to the north, the Atlantic Ocean to the west, and the Mediterranean Sea to the south (figure 1). Lastly, regional climatic contrasts are reinforced by the presence of medium-altitude mountain areas (the Massif Central, Vosges, and Jura) and higher mountain ranges to the southwest and southeast (Pyrenees and Alps). This study omits the island of Corsica, a typically Mediterranean area range with Alpine nuances (Rome and Giorgetti, 2007).

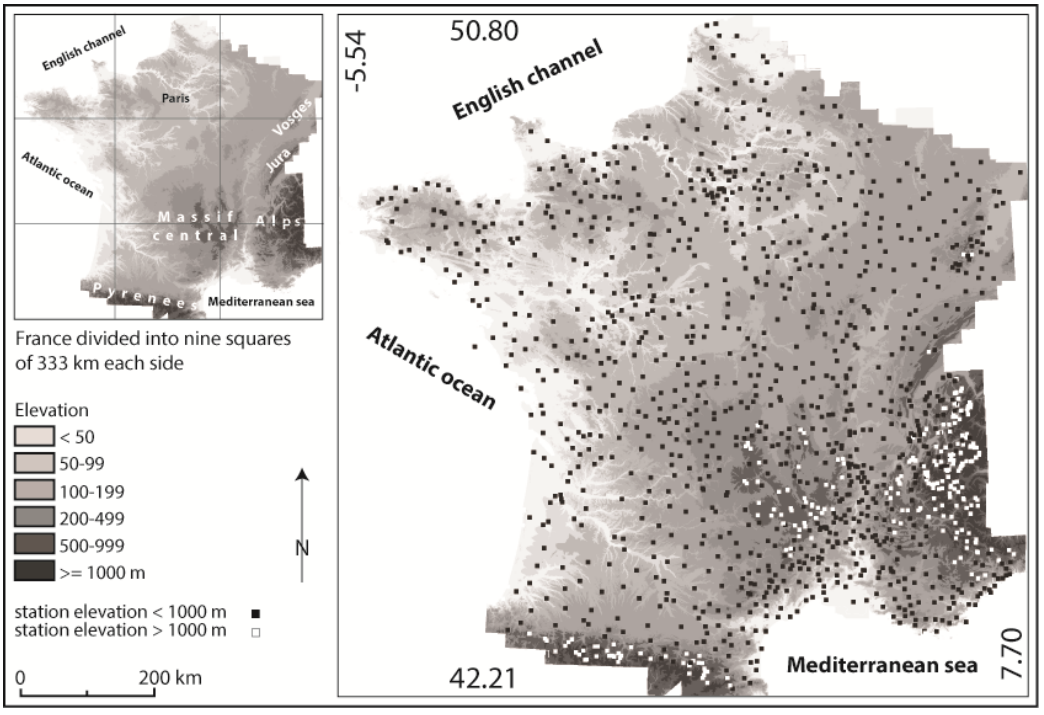

Figure 1. Study area continental (France) and 1098 Météo-France stations. The coordinates are given in degrees in the WGS84 system. *Zone d'étude (France continentale) et 1098 stations de Météo-France. Les coordonnées sont données en degrés dans le système WGS84*.

1.1. Data

Météo-France provided the climatic data used. Temperatures are observed at the standard height of 2 m in accordance with the requirements of the World Meteorological Organisation. The acquisition of such data provides information about shielded temperatures which are different from temperatures in the open air. The critical point, however, is that the acquisition mode is the same as it allows comparison of the recorded data. The time sample used is 10 years: from 1 January 2008 to 31 December 2017 (3653 days). This span is long enough to avoid overdependence on the interannual variability of weather conditions, while maintaining as many stations as possible, given that many stations have been opened or, on the contrary, recently closed. For the 10 years under study, data from 1098 stations were downloaded (figure 1). The data used are the daily minimum (tn) and maximum (tx) temperatures.

1.2. Method

The objective of the procedure is to pair two stations close to each other but with a sufficient difference in elevation to allow significant temperature differences. Each of the 1098 stations of the Météo-France network is potentially the first of a pair of stations: if a match is found for it, it becomes the low station. The statistical algorithm tests each of the other 1097 stations to determine which one can be paired with it. This 'high station' is the closest of the network stations that meet the five criteria set out below. It should be noted that a station may be included in more than one pair.

The objective is (*i*) to obtain enough pairings to provide statistics on inversions (intensity, frequency, and duration) and (*ii*) for these pairings not to omit any region. It should be specified that the term 'pair' is used for the couple formed by two stations, one high and one low, whereas the term 'site' refers to the spatial context formed by a pair of stations.

1.2.1. Station pairing criteria

- **Maximum distance**

We look for the companion station within a given radius for each of the 1097 stations that can potentially be paired with a given station. This maximum distance value can be parameterized: a low value (dist_max < 20 km) reduces the number of potential stations for pairing but increases the climatic coherence of the paired stations; a value exceeding 50 km increases the potential for pairing exaggeratedly while allowing climatologically different stations to be paired.

The value finally attributed to this parameter was 30 km (see section 2.1. '*Pairing characters*' for the explanation of this choice), so that a pair of stations can be selected if the Euclidean distance between them is less than 30 km.

- **Topographical context**

Topography is not involved in identifying the low station. It is used only for determining the high station that must not be in a valley or depression because such sites are prone to cold air drainage and conducive to inversions. Any other context (flat, slope, crest) may be selected.

- **Minimum altitudinal difference**

We use the term altitudinal difference (dif-alt) for the difference in altitude between high and low stations in a pair. We select only high stations that are at least 100 m higher than the corresponding low station (Joly and Richard, 2019). Although this value may seem small, it means no stations along a broad fringe of the Atlantic coast, representing almost half of France, can be paired. Accordingly, the variable 'distance from the sea' is introduced to progressively narrow this difference as we approach the ocean (eq. 1). The minimum altitudinal difference (dif-alt_min) thus varies from 27 m beside the sea to 100 m in the vicinity of Mulhouse, where the distance from the sea is maximum.

$$difalt_{min} = \frac{difalt}{1+log10(dmmax-log10(distmer))} \qquad \text{eq. 1}$$

Where *difalt* = 100 m (minimum altitudinal difference limit imposed); *distmer* = distance from the sea; *dmmax* = maximum distance from the sea (492.5 km).

- **High-station temperature correction**

The altitudinal difference between the stations forming each pair is problematic as Joly and Richard (2018) show: '*The negative relationship between inversion frequency and altitudinal difference is strong for both tn and tx (R = -0.83 and -0.60 significant at the 1% and 5% levels).*' This is because high stations located much higher than the upper limit of the boundary layer cool at a faster rate than the adiabatic temperature lapse rate. A pair in this configuration has much lower inversion frequencies than a pair near the boundary layer.

Suppose we use only the positive values of differences between high and low stations. In that case, we obtain absolute inversions that depend largely on the altitudinal difference between the two stations. To avoid this effect, we identify what are termed relative inversions, for which the temperature of the high station has been reduced proportionally to altitude (eq. 2).

$$TempsTh = TempsTh + \left(\frac{difalt}{100} * ATLR\right) \qquad \text{eq. 2}$$

Where *TempSTh* = the temperature observed at the high station; *difalt* = the altitudinal difference between the high and low station; *ATLR* = the adiabatic temperature lapse rate used in this research (-0.6°C/100 m).

The temperature of the high station must be corrected to bring it thermally to the same altitude as the low station. The correction value (-0.6°C/100 m elevation) selected to correct the high-station temperature (figure 2) is slightly lower than the altitudinal temperature decrease in free air (0.65°C/100 m). Firstly, as mentioned, the temperature is recorded under shelter, not in the open air, leading to biases. Secondly, the air layer near the ground is anything but a free air layer. In actual practice, the situation is extremely complex because the altitudinal lapse rate has multiple contributory factors, notably atmospheric pressure and air humidity. But these variables are measured for a small number of the 1098 stations, which limits any influence. Most of the studies we consulted show that the altitudinal lapse rate varies according to the time of year (Rolland, 2003), the daily maximum and the daily minimum, and that it is close to 0.6°C on average (Dodson and Marks, 1997; Rupp *et al.*, 2020). This is the value we have chosen for this work.

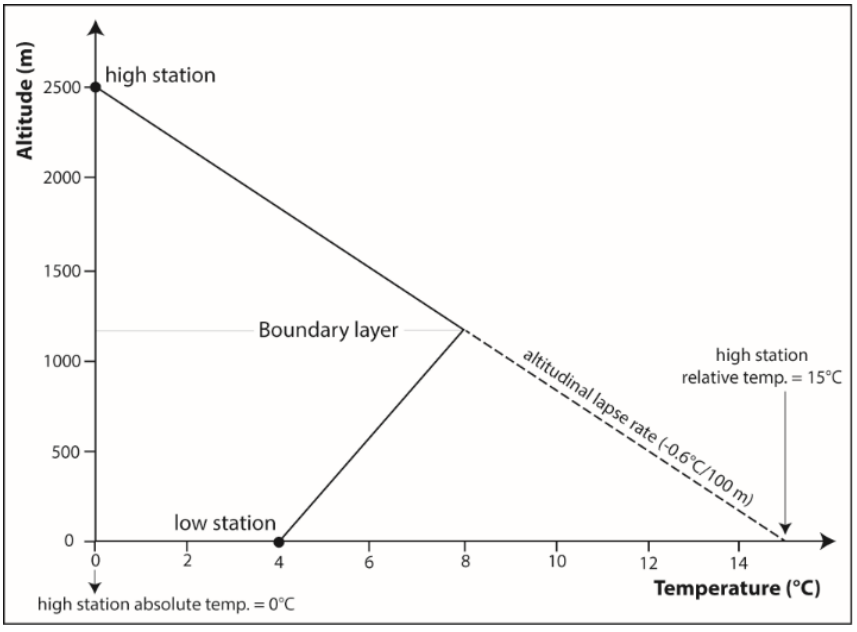

Figure 2. Correction of absolute temperature to yield relative temperature. *Correction de la température absolue pour obtenir la température relative*.

In Figure 2, the sloping dotted line shows what the temperature would be in the absence of the surface inversion. The absolute temperature of the high station is 0°C (4°C lower than the low station). Without the inversion, the low station would have a temperature of 15°C. Applying equation 1 lowers the absolute temperature of the high station by $0 + \left(\frac{2500}{100} * 0.6°C\right)$ meaning that the relative temperature is 15°C, *i.e.* 11°C higher than the temperature at the low station (4°C): that is what we call the 'inversion intensity'.

1.2.2. Analytical methods

The temperature difference is calculated separately for daily tn and tx, and between each pair of stations by subtracting the temperature recorded for the low station from the relative temperature for the high station. A positive result indicates a thermal inversion, with the temperature being higher at the high station than at the low station. Three characteristics are calculated: intensity, frequency, and duration of inversions for each site. Of the three characteristics, intensity is the most straightforward, as it corresponds to the difference in temperature between the two stations of each pairing. An inversion at a single station during a tn or tx is termed a 'point inversion'. There are potentially as many point intensity values as pairs of stations multiplied by the number of days of observation. A mean intensity can also be calculated for each of the 3567 days, 120 months, or 10 years of the period of observation. The frequency of inversions is the number of inversions within a given period (day, month, year).

There are two ways of calculating the duration of inversions. The general principle is to determine how inversions persist over time. The first way is to

identify persistent inversions: a tn-inversion is preceded or followed by a tx-inversion and a tx-inversion is preceded or followed by a tn-inversion (figure 3A). Such inversions are termed 'persistent inversions'. Depending on the persistence of the conditions that cause the inversion and the topography of the sites, these persistent inversions may last for several days or even weeks. The second way is to identify isolated inversions: a tn-inversion is neither preceded nor followed by a tx-inversion, and a tx-inversion is neither preceded nor followed by a tn-inversion. These are termed 'isolated inversions'. Isolated inversions occurring sporadically during a period of non-inversion are termed 'ephemeral inversions' (figure 3B). Where they recur the next day or over several days in succession, they form what are called 'inversion sequences' (figures 3C and 3D). The duration of an inversion sequence or a persistent inversion begins on the first day with an inversion (tn or tx).

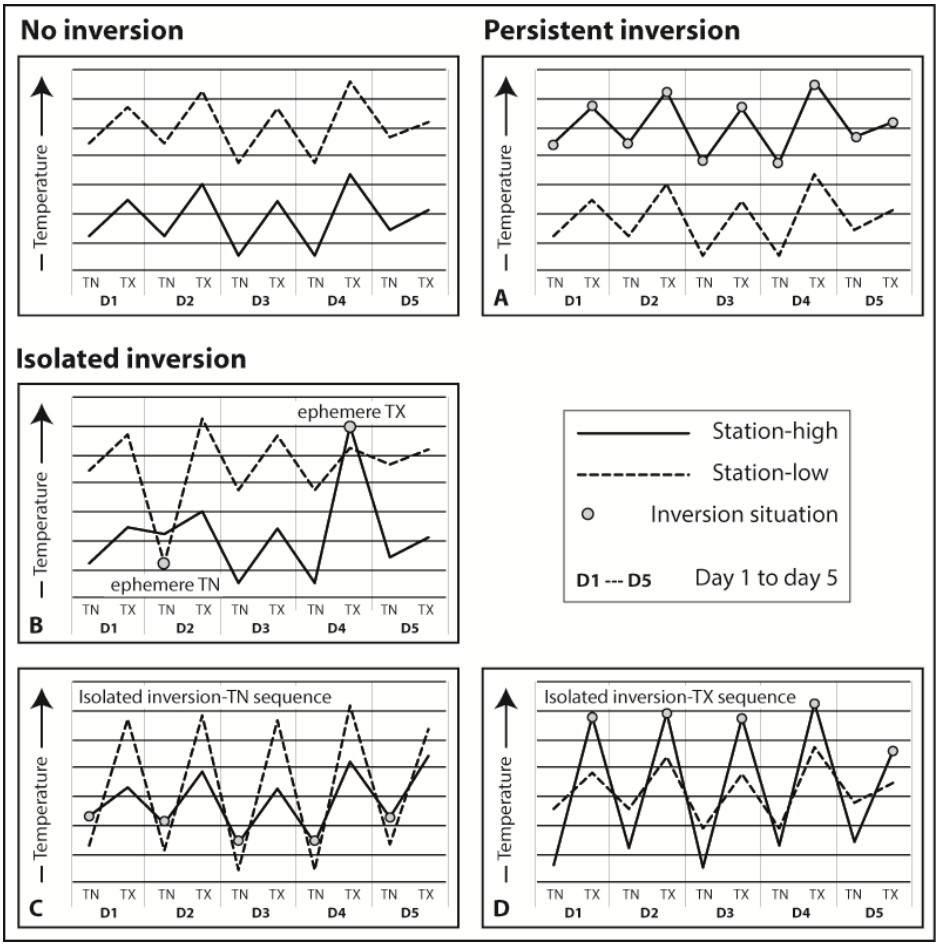

Figure 3. The different types of inversions named in the paper. *Les différents types d'inversion cités dans l'article.*

In most instances, we use classical descriptive statistics. In some cases, regressions are used to estimate values and calculate the slope or the Bravais-Pearson correlation coefficient (R). Other treatments are considered for relating the characters of inversions with daily temperature amplitudes (DTAs) which, as they provide indirect information on radiative conditions (Erpicum, 2004), are considered proxies for atmospheric conditions. Most works on temperature inversions mention that the characteristics of inversions vary with the weather (Dorninger *et al.*, 2011; Vitasse *et al.*, 2017). Westerly advection with cloud, wind, and often precipitation (lowDTA) is not conducive to the formation of inversions and destroys any inversions that may have formed. Conversely, high-pressure areas with cloudless skies (high-DTA) are still conducive to the formation of inversions at night. Because the temperature observed at a weather station depends on radiative and advective influences, the DTA is a good integrator of these atmospheric conditions. The DTAs used are those

recorded at the low station. We do not analyse DTAs measured at high stations where 100% cloud cover may occur during the day, especially in summer when convectional movements are the most intense.

Each DTA value is associated with many situations that present varied occurrences, intensities, and durations of inversions. This diversity produces statistical noise that interferes with the identification of marked trends connecting these two variables (Joly and Richard, 2019). Accordingly, the mean intensity and frequency have been calculated in classes grouping together the DTA values in whole units to reduce this instability. This operation yields 18 statistical individuals characterized by a DTA value class, and a mean intensity and frequency. DTAs also vary with the time of year. Generally, the greatest DTAs are observed in the summertime when direct solar radiation is strongest. To reduce this effect, statistics relating DTA and individual inversions are given for the four seasons: winter (DJF), spring (MAM), summer (JJA) and autumn (SON).

2. Results

2.1. Pairing characters

The dist_max parameter sets the radius of the circle outside which a station cannot be selected as the high station of a pair. A low value, such as 10 km, is optimal climatologically but allows too few pairs (182) before other constraints are applied. With distances of 20 and 30 km, the number rises to 678 and 1524, respectively. We opted for 30 km because it allows a better spatial distribution of pairings across France as a whole. After other constraints (altitudinal difference, high-station topographical context) were applied, the number of pairs came to 1187. These 1187 pairs were formed by 627 separate low stations, meaning that, of the corpus of 1098 stations available, 471 stations did not find a station that satisfied the constraints. To visualize the distribution of pairs, France was divided into nine squares with sides of 333 km. Most pairings are in central and SE France, which is consistent with the relief pattern. The sectors to the north and west have fewer pairings because the relief is less complex and land areas less extensive (the coastal squares include varying amounts of maritime areas).

A final filter was applied and only those stations with a shortfall of less than 10% of temperature readings (tn and tx) were selected. In the end, 328 stations failed to meet this new constraint and a total of 859 pairs were used. These included 302 made up of a low station connected with a single high station (e.g. pairs BC and DE in figure 4). The others were formed from a low station associated with two (AC - AD), three, or more high stations. A single station (C) may serve as the high station for two or more pairs (AC and BC). Lastly, the same station (D) may serve as the high station for one pair (AD) and then the low station for another pair (DE). In Figure 4, the algorithm rejects pairs AE and BE as they are more than 30 km apart.

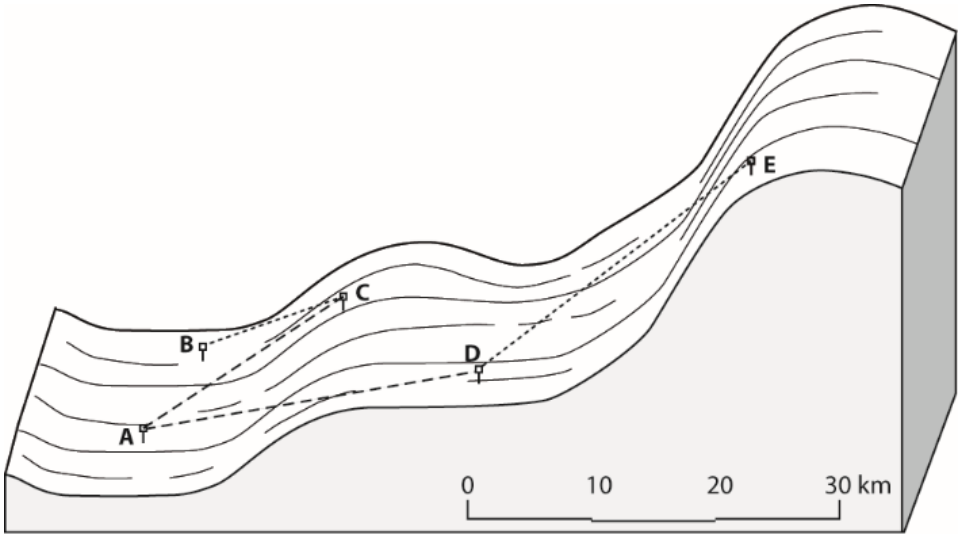

Figure 4. Different types of connection between high and low stations (the letters mark the position of fictitious stations given as examples). *Différents types de liaison entre les stations hautes et basses (les lettres marquent la position de stations fictives données à titre d'exemple).*

The maximum distance between the two stations in each pairing imposed by the algorithm is 30 km, and the minimum distance is 0.8 km (figure 5). The mean distance is 20.3 km, close to the median (21.3 km). Half of the total number falls between 15.7 and 25.8 km. Altitudinal differences are mostly less than 530 m (Q3). Given the altitudinal difference tolerance for pairings close to the coastline, differences of less than 50 m account for 8% of the total. The maximum is 2333 m, while 7% of pairs have a difference of more than 2000 m and just 0.4% (5 pairs) exceed 2000 m.

The high stations are, on average, 300 m higher than the low stations with a wide dispersion. The elevation of the low stations is less than 600 m for more than 75% of the sample, but even so, some of them (20% of the sample) are in mountain areas at altitudes of more than 2000 m.

The topographical context supports the idea that the high stations are located on prominent relief with altitudinal differences exceeding 65 m in 50% of cases and 200 m in 25% of cases, with the maximum being 882 m. Conversely, the low stations are in gentle relief or at the bottom of valleys or shallow hollows. The negative reliefs within which the low stations are found are moderate (75% less than 200 m), and the positive reliefs are barely prominent (75% less than 21 m).

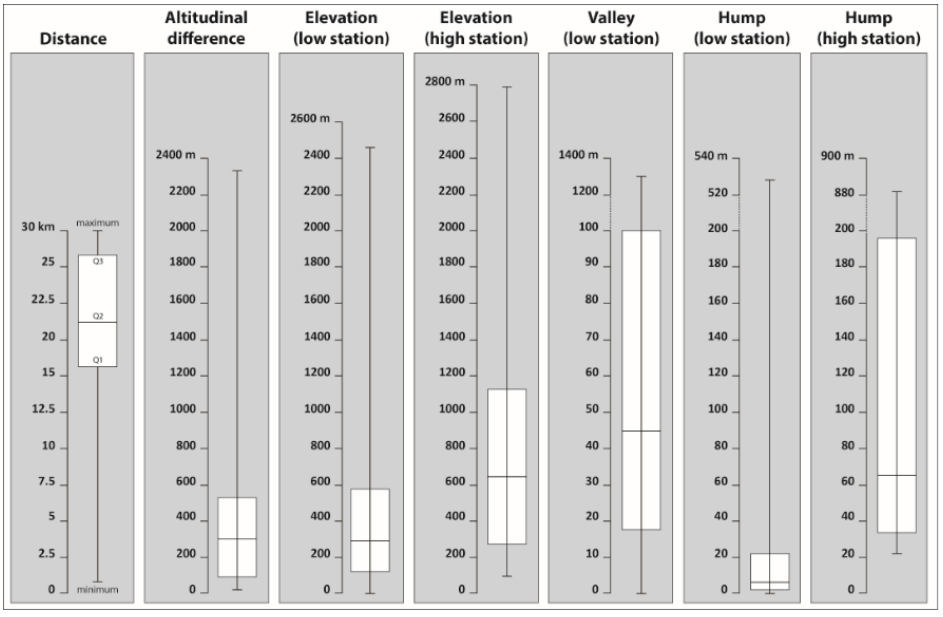

Figure 5. Box plot of morphometrical characteristics of pairs of stations. *Boîte à moustaches des caractéristiques morphométriques des paires de stations.*

2.2. Descriptive statistics of intensity, frequency, and duration of inversions

2.2.1. Intensity of inversions

Each of the 1 975 597 (tn) and 835 345 (tx) point inversions recorded is characterized by a value, its intensity, which indicates the deviation between the high and low stations. The maximum point intensity recorded at night-time (tn) was 23.6°C in the Alps east of Grenoble on 7 February 2011 (figure 6A). The two stations concerned are separated by a difference in altitude of 843 m, the low and high stations being at an elevation of 886 m and 1729 m, respectively (values given by geomatics). The low station (La Mure) is located at the bottom of a 221 m deep valley. In contrast, the high station (Chamrousse), located at the top of a slope about 100 m from the summit, emerges at 633 m above the local average topographic plane. A stable anticyclonic situation with pressures exceeding 1030 hPa settled over the Alps during the first week of February 2011. The weather is sunny, with temperatures in the valley ranging from -5°C with a relative humidity close to 100% at 9 am (tn) to 15°C at 3 pm (tx). This high value contrasts with the high percentage of low intensities (Q1, median, and Q3 = 0.8, 2, and 3.9°C). The fact is that a very marked intensity, of more than 10°C, occurs for only 1.4% of the corpus.

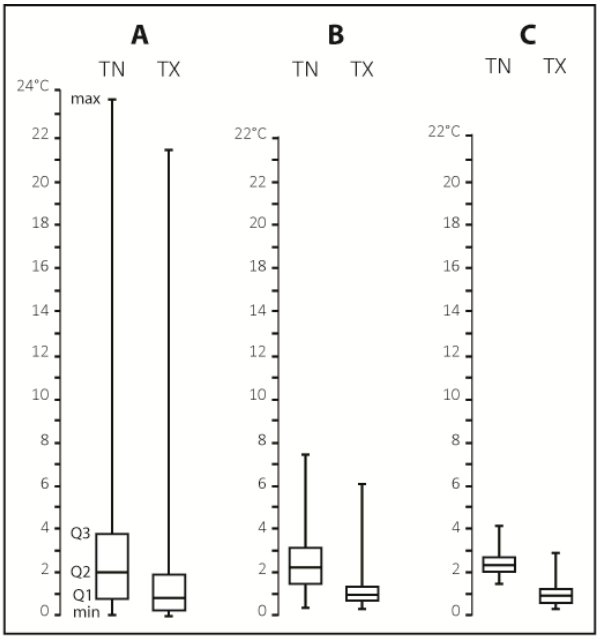

Figure 6. Box plot of inversion intensity; A: episodic, B: daily, C: monthly. *Boîte à moustaches de l'intensité des inversions avec : A = ponctuel, B = quotidien, C = mensuel.*

The maximum intensity recorded for the daytime (tx) is 22.6°C. The value is similar to that of tn. It occurred on 1 January 2015 at a site in the Alps 80 km NE of Grenoble. The two stations concerned are separated by a difference in altitude of 2302 m, the lower and upper stations being at an elevation of 480 m and 2782 m, respectively. The low station (Moûtiers) is in the heart of the town at the bottom of a deep valley. The high station (La Masse), located on a mountain ridge, emerges at 503 m above the average local topographic plane. During this maximum, the situation is again anticyclonic (1035–1040 hPa), sunny, moderately cold in the morning (-1°C), and mild in the afternoon (5°C). The relative humidity is 50% at 3 pm during the tx. Intensities of more than 10°C make up just 0.8% of the sample.

A mean intensity can also be calculated for the 3567 days from the 859 station pairs covering the whole country. The highest mean daily intensity is 7.5°C for tn (7 February 2011) and 6.1°C (9 January 2013) for tx (figure 6B). The central tendency values exhibit low dispersion and are about twice as high for tn as for tx. The same applies for the mean monthly intensities (figure 6C) where the maximum recorded is higher (4.3°C for tn and 3.1°C for tx).

The mean monthly intensities vary little for tn (2.2°C to 2.8°C) and do so in a way that contrasts summer (0.7°C) and winter (1°C to 2°C) for tx (figure 7A). Although caution is required given the short span of the period (10 years), the trend that appears is for intensities to increase; $R^2 = 0.10$ and 0.35 for tn- and tx-inversion intensities (figure 7B).

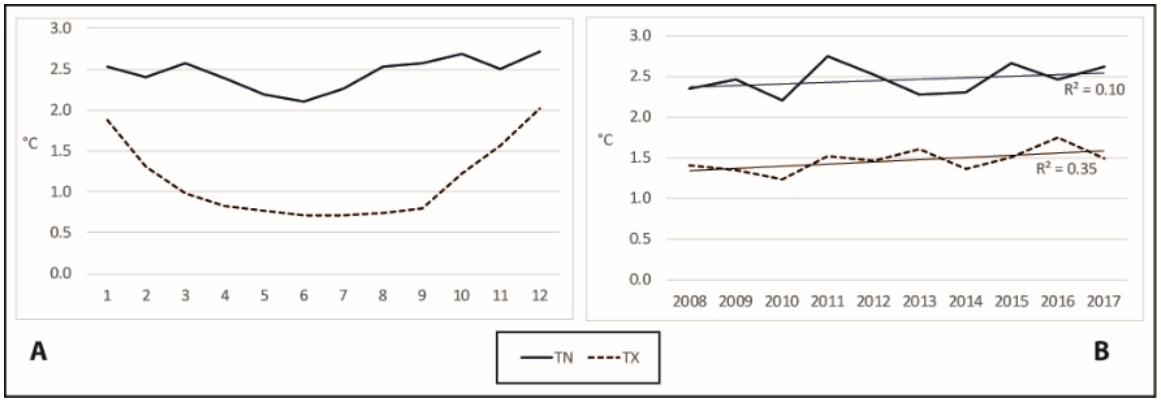

Figure 7. Variation in intensity of inversions. A: over the year (12 monthly means) B: over the observation period (annual means). *Variation de l'intensité des inversions. A : sur l'année (moyennes sur 12 mois). B : sur la période d'observation (moyennes annuelles).*

This trend is significant for tx-values alone and only at the 10% level. It is associated with an increase in temperatures. The short span of years means we cannot draw any general conclusions. Even so, the link between higher temperatures and frequent inversions raises questions. This may be linked to the relative sheltering from climate change of valley bottoms vs exposed peaks. The latter are coupled much more strongly with the free air and thus influenced by climatic changes in free air temperature. Valley bottom temperatures under an inversion are additionally linked to radiative processes and sub-surface temperatures and so less directly influenced by changes in free air temperature (Pepin and Norris, 2005; Pepin and Seidel, 2005; Mountain Research Initiative EDW Working Group, 2015).

2.2.2. Frequency of inversions

Frequency is the number of inversions compared with the total number of inversions over a given period. Considering the entire observation period, 3 137 927 units (859 pairs over 10 years) are counted. For tn and tx, 1 975 597 and 835 345 point inversions are identified, respectively. Inversions occur on 63% of nights and 22.6% in the daytime.

For each of the 3657 days, occurrences of inversions vary from 0 (no inversions across the study area) to 859 (all sites observe an inversion). The day with the maximum number of inversions at the time of tn (764 or 88.9% of the sample) is 20 August 2011 (figure 8).

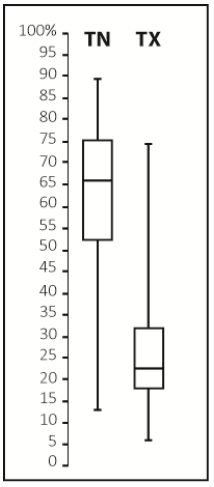

Figure 8. Box plot of tn and tx inversion frequency at daily scale (3657 days from 1 January 2008 to 31 December 2017). *Boîte à moustaches de la fréquence des inversions tn et tx à l'échelle quotidienne (3657 jours du 1er janvier 2008 au 31 décembre 2017).*

The day with the most tx-inversions is 3 December 2013 with 641 sites concerned (74.6%). Quartiles 1 and 3 are respectively 52% and 76% for tn and 18% and 32% for tx.

Inversion frequency patterns over the year (12 monthly averages) differ plainly between tn and tx (figure 9A). The most frequent simple night-time inversions (tn) occur in late summer (August) and early autumn (September to October). They are rarest in February and overall, in the first half of the year (January to June). This maximum frequency in late summer is a statistic that is inconsistent with what is commonly perceived and even with the image given by various media.

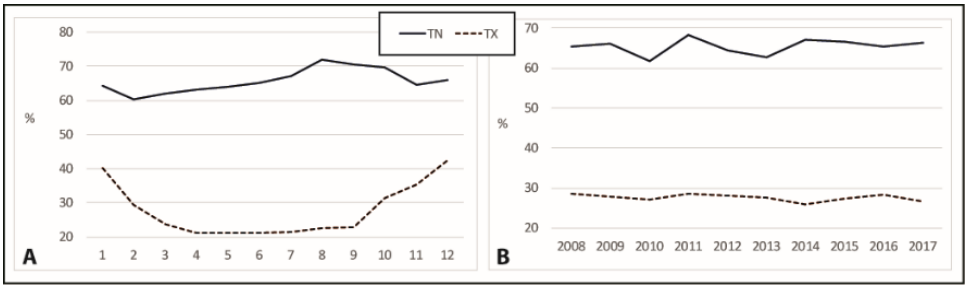

Figure 9. Variations in inversion frequency. A: throughout the year 12 (monthly means). B: over the period of observation (annual means). Variations de la fréquence des inversions. A : tout au long de l'année (moyennes sur 12 mois). B : sur la période d'observation (moyennes annuelles).

The intra-annual variation in tx frequency is identical to that of tx intensity: low frequency in summer (20%), and higher frequency in winter (40%). Lastly, it is true that frequencies show no trend over a short span of time (10 years), whether for tn- or tx-inversions (figure 9B).

2.2.3. Duration of inversions

Cases of tn-inversions are almost equally divided between isolated sequences and persistent inversions. About one tn-inversion in two (53%) is destroyed during the day. Conversely, most tx-inversions (81%) are persistent inversions. Only 19% of tx-inversions are isolated sequence inversions, that is, they are destroyed in a night.

Examination of the duration of sequences shows that 45% of isolated tn-inversions and 75% of isolated tx-inversions are ephemeral (figure 10). Generally, isolated tn-inversion sequences last longer than isolated tx-inversion sequences. Thus, the proportion of tn-inversion sequences lasting at least 10 days is 7% versus 0.3% for tx-inversion sequences. The maximum duration of isolated tn-inversion sequences is 126 days. This event occurred in the summertime, from 6 June to 9 October 2011, in the hinterland of Nice (close to the Mediterranean Sea). The maximum duration of isolated tx-inversion sequences is 38 days. This event occurred in spring at the mouth of the Seine River, near Le Havre (close to the English Channel), from 9 April to 16 May 2017 when the temperature difference between the cooler sea and warmer land was particularly large.

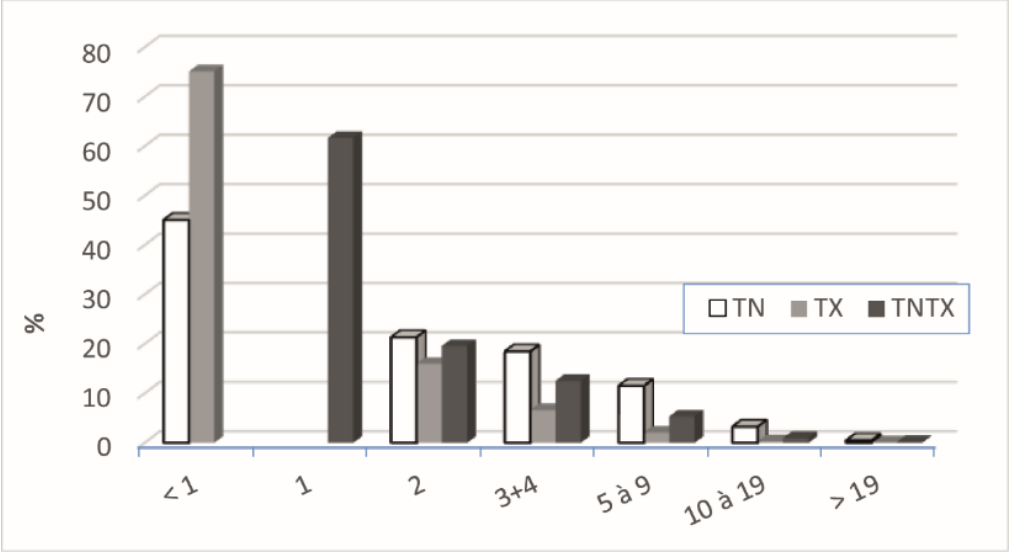

Figure 10. Frequency as a function of duration of inversions (days). White (TN), isolated tn-inversions; grey (TX) isolated tx-inversions; black (TNTX) persistent inversions. *Fréquence de la durée des inversions (en jours). Blanc (TN), inversions tn isolées ; gris (TX) inversions tx isolées ; noir (TNTX) inversions persistantes.*

A study of the duration of persistent inversions shows that, here, the majority (60%) are one-day persistent inversions, while just 19.5% last for two days, then 12.5% for three successive days, etc. Only 1% of persistent inversions last for more than 10 days, with the maximum being 88 days in winter from 28 November 2013 to 23 February 2014 in the Alps near Grenoble. These extended sequences of persistent inversions are formed during stable anticyclonic situations. Figure 11 seeks to characterize the seasonal variation in the duration of the three different types of inversion. In winter, most tn-inversions can be classified as uninterrupted inversions lasting from several days to several months. The persistent inversions then last longer (2.5 days) than the isolated tn-inversion sequences (1.5 days) (figure 11A). In the summertime, uninterrupted inversions are rare, resulting in isolated tn-inversions lasting longer (3.5 days) than persistent inversions (1 day). The opposite can be observed with isolated tx-inversion sequences not marked by a cyclical change with the seasons.

There is no significant variation in the duration of inversions over the period of observation (figure 11B).

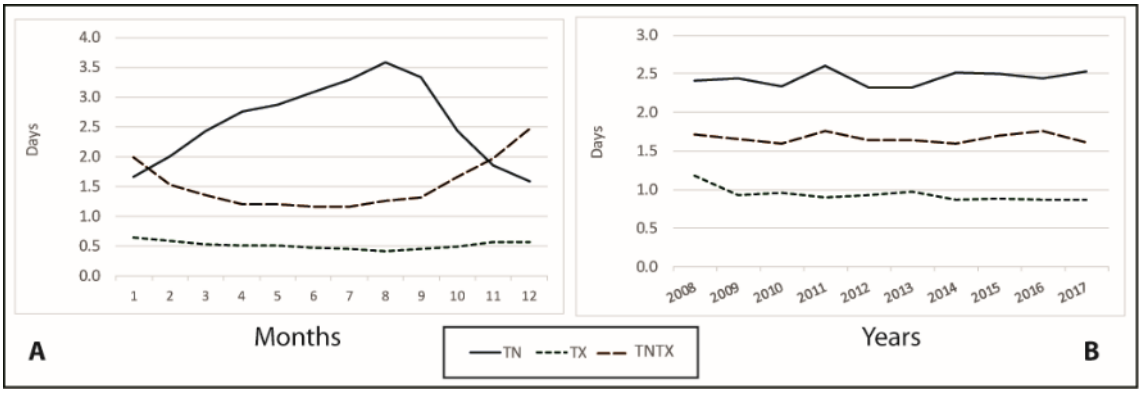

Figure 11. Variation in the duration of inversions. A: over the course of the year (monthly means); B: over the period of observations (annual means). TN= isolated tn-inversions; TX= isolated tx-inversions; TNTX= persistent inversions. *Variation de la durée des inversions. A : au cours de l'année (moyennes mensuelles) ; B : sur la période d'observation (moyennes annuelles). TN= inversions tn isolées ; TX= inversions tx isolées ; TNTX= inversions persistantes.*

2.3. Typology

The objective of this section is to propose a synthetic approach to inversions. This involves analysing by Ascending Hierarchical Classification (AHC) the relations between simple tn- and tx-inversions and the indicators that characterize them: intensity, frequency, and duration. Here the AHC classifies each of the 3653 days by seven characters: mean daily intensity of tn and tx, mean daily frequency of tn and tx, number of days in a row with ephemeral tn- and tx-inversions, and duration of inversions. Three classes are required. AHC is based on Euclidean distance and Ward's method. The statistics of the variables are given in Table 1.

Table 1. Descriptive statistics of the variables introduced in the Ascending Hierarchical Classification (AHC). TN and TX = tn- and tx-inversions; Frq = frequency (%); Intens = intensity (°C); Seq = duration of sequencies of isolated inversions (days); PersTNTX = duration of persistent inversions (days). *Statistiques descriptives des variables introduites dans la classification hiérarchique ascendante (CHA). TN et TX = tn- et tx-inversions ; Frq = fréquence (%) ; Intens = intensité (°C) ; Seq = durée des séquences d'inversions (jours) ; PersTNTX = durée des inversions persistantes (jours).*

Variable	Minimum	Maximum	Mean	Stand. deviation
Intens-TN	-20.4	50.6	24.3	11.6
Intens-TX	-8.3	48.5	12.0	7.1
Frq-TN	-49.9	26.0	63.0	15.8
Frq-TX	-20.3	48.0	26.6	12.2
Seq_TN	-12.4	44.4	13.0	9.7
Seq_TX	-0.6	2.0	0.7	0.3
PersTNTX	-4.7	38.9	5.2	4.8

Class 1 contains 17% of the 3653 days studied. It is characterized by the intensity, frequency, and duration of persistent inversions that are very well above the mean (table 2). Only sequences of isolated tn-inversions are clearly below average. Class 1 occurs in winter only, with its maximum value in December (figure 12). The assumption is that it occurs during rather lengthy periods of cold anti-cyclonic weather when the intense inversion cannot be destroyed in the day.

Class 3, with 51% of days, contains individuals characterized by a high frequency of tn-inversions (71.7%), comparable with class 1 (table 2). These inversions are seldom persistent but give rise to long isolated tn-inversion sequences (19.2 days). These are weak inversions at the night's end that occur in all seasons except in winter, where they are rare (figure 12). They are most frequent in late summer (August and September). The duration of isolated tn-inversion sequences reflects the persistence of

weather conditions leading to the repeated night-time formation of inversions destroyed over the day. This type of inversion presupposes that conducive weather conditions or anti-cyclonic conditions in the warm season or at the end of the warm season are commonplace.

Table 2. Average values of the seven characters in each of the three classes. Day=attribution of days by class. TN and TX = tn- and tx-inversions. Intens. = intensity. Freq. = frequency. Seq. = duration of the sequences of isolated inversions. Pers. TNTX = duration of persistent inversions. Bold value > mean. *Valeurs moyennes des sept caractères de chacune des trois classes. Day = nombre de jours par classe. TN et TX = tn- et tx-inversions ; Frq = fréquence (%) ; Intens = intensité (°C) ; Seq = durée des séquences d'inversions isolées (jours) ; PersTNTX = durée des inversions persistantes (jours). valeurs en gras > moyenne.*

Class	Day (%)	Intens. TN (%)	Intens. TX (%)	Freq. TN (°C)	Freq. TX (°C)	Seq. TN (days)	Seq. TX (days)	Pers. TNTX (days)
1	17	3.4	2.4	72.1	48.6	5.6	0.6	**12.6**
2	32	1.4	0.9	44.3	21.5	7.0	0.7	3.1
3	51	2.8	1.0	71.7	22.5	**19.2**	0.7	4.1
	Mean	*2.4*	*1.2*	*63.0*	*26.6*	*13.0*	*0.7*	*5.2*

Class 2, 32% of days, has below-average values for all indicators (table 2). These are preferentially days when, on average, in France, inversions are not intense and below average in frequency and duration. This class occurs throughout the year but slightly more in winter and spring and slightly less in late summer. The assumption is that it corresponds to disturbed weather conditions with wind and rain that are not conducive to inversions.

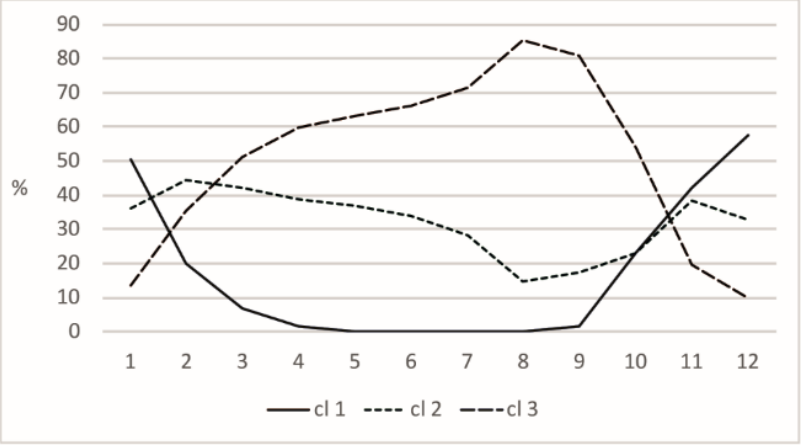

Figure 12. Percentage variation in the three types of inversion over the 12 months of the year. *Variation en pourcentage des trois types d'inversion au cours des 12 mois de l'année.*

3. Discussion

3.1. Limitations of the method

The further apart the two stations of each pair are, the more the temperature characteristics at a given time may be influenced by different factors. This is particularly true in the Alps, where the peaks may be covered with clouds while the valleys are sunny. Another source of error is that minima or maxima do not necessarily co-occur at the low and high stations. For example, the valley bottoms may receive the first rays of the sun later at sunrise than the neighbouring peaks and vice versa in the late afternoon. So, the temperature difference at a given time between these two places could be smaller than that calculated. It was impossible to quantify the impact of these two sources of error on the characteristics of the inversions because we only have the daily tn and tx temperature records. But, except for the Alpine valleys, the time difference between the minimum or maximum at the two stations is likely to be small, a few hours at most, and at a time when temperature variations are usually minor. The minimum at the low station may occur before or after the minimum at the high station. Thus, the positive deviations counterbalance the negative divergences so that, statistically, the

impact of the error over the ten years of the study is probably low. It would be necessary to acquire additional data such as cloud fraction or hours of sunshine and to use fine-grained records to find out more.

Another point is worth discussing. It is hard to determine whether the chosen gradient value biases the results. If the gradient of 0.6°C/100 m is systematically wrong, then one would expect, even under well-mixed conditions (no inversion), that an inversion or a superadiabatic difference would be detected, depending on whether 6°C/km is too large or too small. This could happen in cases where the temperature differences are minimal. At the same time, the vertical variation of temperatures for large and small altitudinal differences cannot be compared to verify that the chosen lapse rate is correct, as the inversion characteristics vary according to topographical features (Sheridan, 2019). The only way to check this would be to analyse the high-resolution temperature and humidity profiles to determine the typical effective value of the wet lapse rate, reflecting the specific background humidity. Even then, so many factors affect this phenomenon in different regions and under different climatic regimes that an in-depth study would be needed to make statements with any degree of assurance. We cannot carry out such a study.

3.2. Temperature correction

The characters of inversions were determined from temperatures corrected for the elevation effect to allow for the temperature lapse rate that disrupts the identification of inversions, especially when there is a significant difference in elevation between the high and low stations (section 1.2.1.). In this case, inversions are 'relative' as opposed to 'absolute' when the actual uncorrected temperature is higher at the high station (El Melki, 2007). This section tests the sensitivity of inversion analysis to this correction procedure. The results obtained without and with correction are compared.

As expected, near-identical results for both forms of computation applied to tn-inversions for slight differences in altitude (figure 13A). However, the deviation increases logarithmically as altitude increases: for sites with differences in elevation between two stations of more than 1600 m, the frequency of relative and absolute inversions is 77% and 12%, respectively.

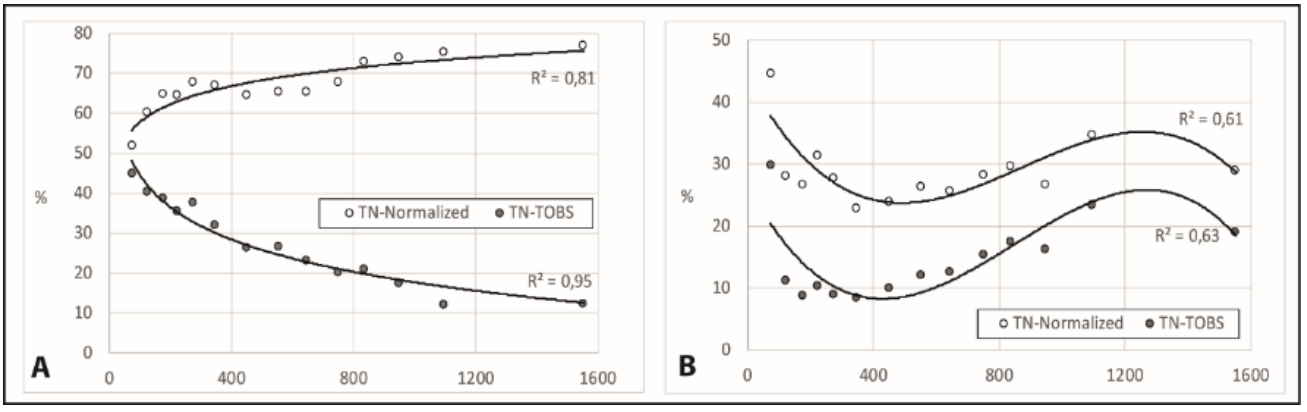

Figure 13. Scatter plot between altitudinal differences in meters (x-axis) versus (A) tn-inversion frequency and (B) tx-inversion frequency according to whether the high station temperature is corrected (TN-Normalized) or not (TN-Obs.). *Diagramme de dispersion entre les différences altitudinales en mètres (axe des abscisses) en fonction de A) la fréquence des inversions tn et B) la fréquence des inversions tx selon que la température de la station haute est corrigée (TN-normalized) ou non (TN-Obs.).*

This latter frequency is abnormally low or even unrealistic, given studies on inversion in Alpine valleys (Fallot, 2012; Kirchner *et al.*, 2013; Largeron and Staquet, 2016a, 2016b). The survey of several Alpine sites revealed that when calculations are based on observed temperatures, the frequency of inversions is low, sometimes close to zero. In contrast, with the correction of high station temperatures, the frequency of inversions rises to 70%. The altitudinal difference is a decisive explanatory factor for frequency, as indicated by the R^2 linking these two variables.

The situation is radically different with the two methods of calculating inversions applied to tx-inversions (figure 13B). The deviation in frequency of inversions is roughly parallel but undergoes a sine-wave variation with the value of the altitudinal difference that the topographical context can explain. Small differences are mostly found beside the sea and in lowlands, whereas large differences are typical of high mountain areas, which are two radically different environments (not illustrated).

3.3. Relation between intensity and frequency of inversions

A strong relationship (R^2=0.72) links the intensity and frequency of inversions. Both indicators show higher values in late rather than early summer (figures 7a, 9a). Another remark concerns the intensity of inversions, which vary similarly to frequencies, but with one nuance: winter inversions, in proportion to those in summer, are more intense than frequent. Two explanations may be suggested. The first is related to the duration of nights. Perhaps the long nights in winter increase the intensity of the inversions but not their frequency, the latter being explained by the former reason related to the vertical stratification of the atmosphere. The oceans and air masses above them heat up during the summer, unlike the land surface, with its very low inertia. Therefore, the air in contact with the landmass cools whenever radiative conditions allow it to, and the inversion forms because the overlying air remains warmer. Simple daytime inversions (tx) are most frequent in December and January. February and November are also often when daytime inversions occur, and their winter character is thus demonstrated.

3.4. Relation between intensity, frequency of inversions and daily amplitude of temperatures

Regional climate and weather conditions are a decisive explanatory factor for the variation of inversions over time (Joly and Richard, 2019; Rupp *et al.*, 2020). To capture this influence, we utilize DTA (daily temperature amplitude) observed at the low station of each pair (section 1.2.2.).

The tn-inversion intensities are linked to DTA. But the connection is not a constant one (figure 14A). Tn-inversion intensities are very low, less than 1°C, for DTAs less than 3°C. They rise steadily to a value of 10°C. Then the increase becomes sharper with the intensity for DTAs of more than 18°C reaching 6°C. There is practically no change in tx-inversion intensities with DTAs. This point requires some comment. It is unsurprising that Tn-inversions, generally based on clear and calm conditions, are more intense and frequent in these high DTA conditions. The behaviour of Tx inversions, which respond only slightly or in the reverse direction, is surprising. This can be explained by the occurrence of Tx-inversions preferentially during subsidence inversions (Joly and Richard, 2019). In this case, low-stratus clouds and/or fog are present over the plains and the valley bottoms, while sunshine and high temperatures prevail at higher altitudes. These situations are frequent in autumn and winter.

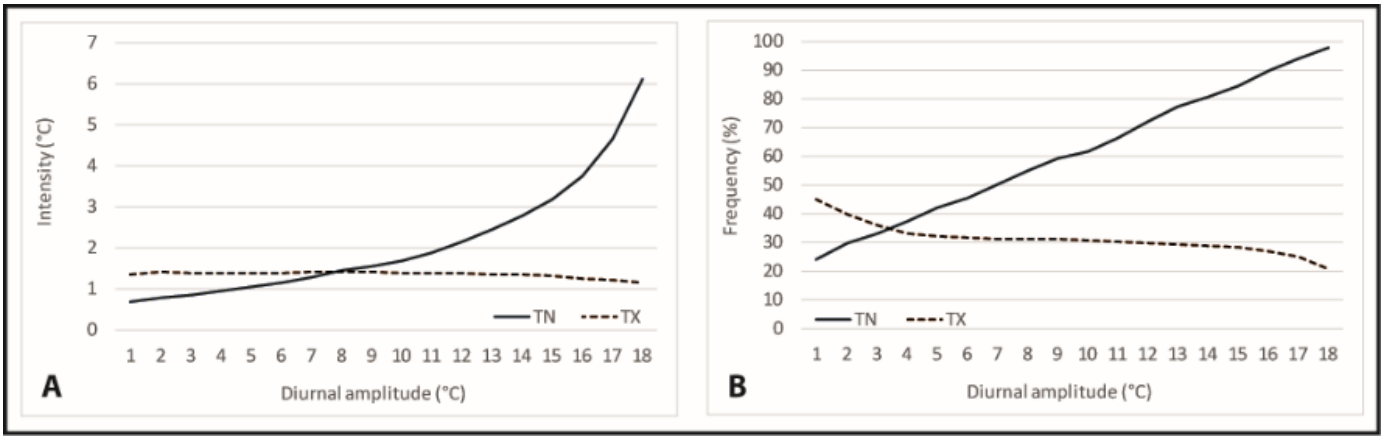

Figure 14. Daily thermal amplitude at the low station at the time of tn and tx versus (A) intensity and (B) frequency (%) of inversions. *Amplitude thermique journalière à la station basse au moment de tn et tx en fonction A) de l'intensité et B) de la fréquence (%) des inversions.*

A near-perfect positive linear connection ties DTA to the frequency of tn-inversions (figure 14B). When the DTA is small, inversions are infrequent. Inversion frequencies track the rise in DTAs to reach a value close to 100% for DTAs of more than 18°C. In contrast to tn-values, a negative relationship is observed for tx-values. The frequencies of tx-inversions are high when the DTAs are small. They decline non-linearly as DTA increases.

3.5. Relation between inversion intensity and duration

It has been possible to associate inversion intensities and frequencies with the DTA because these are sporadic phenomena over time. This is not true of durations which, by definition, last over time. In this case, DTAs correspond to means including a variable number of daily values. Accordingly, comparing DTAs and duration of inversions, the result tends towards a central value with slight variance, which is not optimal for identifying their correlation. For this reason, the duration of inversions is associated with another character, the mean intensity of inversions across each sequence (figure 15). The positive relation between intensity and duration of inversions is borne out for the tn- and tx-inversion sequences and persistent inversions. Whatever the duration, the intensity of inversions in tn-sequences is more significant than that observed for tx-sequences. Intensity for persistent inversions is in-between.

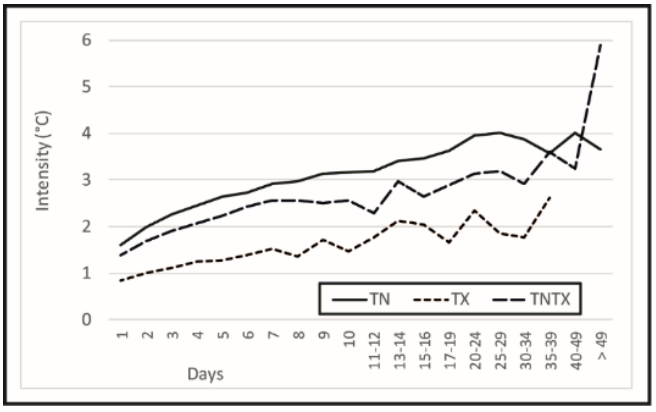

Figure 15. Relation between intensity and duration of inversions. TN and TX = tn-, tx-inversion sequences. TNTX = persistent inversions. *Relation entre l'intensité et la durée des inversions. TN et TX = séquences de tn-, tx-inversions. TNTX = inversions persistantes.*

3.6. Altitudinal temperature lapse rate

Many researchers have suspected that the influence of inversion frequencies might explain the variation in the altitudinal temperature lapse rate (*i*) in the same location between seasons (Rolland, 2003; Kirchner *et al.*, 2013) and (*ii*) between different sites in the same country (Antonioli *et al.*, 2016; Gardner *et al.*, 2009; Joly *et al.*, 2018; Li *et al.*, 2013; Nigrelli *et al.*, 2017). To clarify this, we computed, for each of the 3653 days of observation, the mean Altitudinal Temperature Lapse Rate (ATLR), which is established between the two stations of each of the 859 pairs of stations. At the same time, we have a daily frequency and intensity of inversions. Figure 16, which has as many points (3653) as there are days of observation, plots ATLR against the frequency of tn- and tx-inversions.

The relation observed between frequency and the ATLR is strong, positive, and non-linear (Figure 16A and B). The R^2 values resulting from a third-order (tn-inversions) and second-order (tx-inversions) polynomial adjustment show that the variance of ATLR values is explained by the frequency of tn-inversions (R^2=0.87) and tx-inversions (R^2=0.92). The shape of the two-point clouds indicates an accelerated increase in ATLR values when the inversion frequency exceeds about 60% (tn and tx). Inversion frequency is an excellent proxy for mean daily ATLR values.

Conclusion

A network of 859 pairs of weather stations covering mainland France was used to study the characteristics of thermal inversions. Given the criteria involved in the location of each pair of stations, the modal horizontal and vertical distance between them is 22 km and 300 m respectively. However, in some instances, differences in elevation may exceed 2000 m.

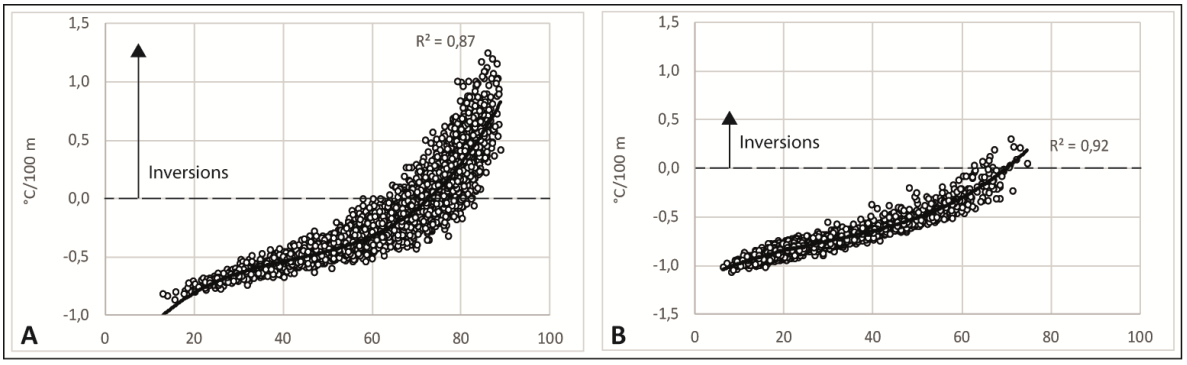

Figure 16. Scatter plot of altitudinal temperature lapse rate °C/100 m (y-axis) versus inversion frequency. Each dot represents one of the 3653 days of the observation period 2008–2017. Frequency (%) of (A) tn-inversions and (B) tx-inversions. *Diagramme de dispersion du gradient thermique altitudinal °C/100 m (axe des ordonnées) en fonction de la fréquence des inversions. Chaque point représente l'un des 3653 jours de la période d'observation 2008-2017. Fréquence (%) de A) tn-inversion et B) tx-inversion.*

The typical topographical context in which the high station is located (low rise) differs from that of the low station (shallow valley). The study concerns the 3653 minimum and maximum daily temperatures recorded between 1 January 2008 and 31 December 2017. Temperatures for the high station were corrected since, in pairs with substantial elevational differences, the difference between the air at the two locations, using absolute temperature. This correction makes it possible to measure the inversion.

The main conclusion is that there is a double contrast between the characters of tn- and tx-inversions and the second winter and summer inversions. The medians of intensities of tn-inversions are higher (2°C) than the medians of tx-inversions (1°C). Far higher values may be observed: 24°C for maximum tn-inversions and 22°C for tx-inversions. The most significant intensities occur in winter, contrasting with the lower intensities of summertime, a typical pattern for both types of inversion (tn and tx). Inversion frequencies are three times higher for tn (65%) than tx (23%). Tn-inversions occur mostly in late summer and autumn, whereas tx-inversions are commonest in winter. The duration of isolated tn-inversion sequences is longer than that of isolated tx-inversion sequences. It is worth pointing out that even on days not conducive to inversions, no part of the country is free from inversions. Conversely, when weather conducive to inversions prevails over all of France, almost 90% (tn) and 75% (tx) of sites experience inversions. Lastly, in terms of frequency or duration, there is no marked tendency in inversions over the ten-year observation period (2008–2017).

The second important point is the close relation between inversions and (*i*) weather conditions and (*ii*) ATLR. High-pressure periods when the atmosphere is dry and still are accompanied by high daily thermal amplitudes (DTAs) that promote the occurrence of radiative inversions that become generalized and intense. However, when the weather is disturbed, DTAs are low because the weather is cloudy or windy, and inversions are scarce. ATLR increases with the frequency of inversions.

Variations of the three inversion indicators (intensity, frequency, and duration) over time are inseparable from the spatial dimension. France is large and climatologically complex enough to present marked differences on the same day. In one place, generalized inversions may prevail while atmospheric conditions may differ elsewhere, resulting in inversions remaining confined to sheltered sites or vanishing entirely. This is a fact that cannot be escaped. While the approach to inversions over time has yielded satisfactory results because the statistics used have made it possible to bring out patterns. But the detailed situation is far more complicated. This can be understood through the rare instances when the maximum frequencies or intensities have been reconstructed spatially. It seems that places or regions are conducive to the formation of high intensities or durations (Alps) while others facilitate long series of tn-inversions (Côte d'Azur) or tx-inversions (English Channel).

This accredits the idea that space structures inversions as much as time does. Current research deals with analysing this spatial aspect to determine whether, for example, the three classes of inversions are evenly distributed throughout France or whether, on the contrary, a particular type is more specific to a particular region.

Acknowledgments: We are grateful to Météo-France for making the data available under the agreement signed with the University of Burgundy.

References

Anquetin S., Guilbaud C., Chollet J.-P., 1998. The formation and destruction of inversion layers within a deep valley. *J. Appl. Meteor*., 37: 1547-1560.

Antonioli S., 2016. *Lapse rate inversions in the Po valley: A 30-year overview*. Master 'Environmental and Land Planning Engineering', Polytechnico Milano, 97 p

Arduini G. Chemel C., Staquet C., 2020. Local and non-local controls on a persistent cold-air pool in the Arve River Valley. *Quarterly Journal of the Royal Meteorological Society*, 146: 2497-2521. https://doi.org/10.1002/qj.3776

Barry R. G., 2008. *Mountain Weather and Climate*. 3rd ed. Cambridge University Press, 506 p.

Bailey A., Chase T. N., Cassano J. J., Noone D., 2011. Changing temperature inversion characteristics in the U.S. Southwest and relationships to large-scale atmospheric circulation. Journal *of Applied Meteorology and Climatology*, 50(6): 1307-1323.

Bish M. D., Guinan P. E., Bradley K. W., 2019. Inversion climatology in high-production agricultural regions of Missouri and implications for pesticide applications. *Journal of Applied Meteorology and Climatology*, 589: 1973-1992. https://doi.org/10.1175/JAMC-D-18-0264.1

Burns P., Chemel C., 2015. Interactions between downslope flows and a developing cold-air pool. *Boundary-Layer Meteorology*, 154: 57-80.

Chemel C., Arduini G., Staquet C., Largeron Y., Legain D., Tzanos D., *et al*., 2016. Valley heat deficit as a bulk measure of wintertime particulate air pollution in the Arve River Valley. *Atmos. Env.*, 128: 208-215.

Conangla L., Cuxart J., Jiménez M. A., Martínez-Villagrasa D., Ramon J., Tabarelli M. D., Zardi D., 2018. Cold-air pool evolution in a wide Pyrenean valley. *Int. J. Clim.*, 386: 2852-2865. https://doi.org/10.1002/joc.5467

Czarnecka M., Nidzgorska-Lencewicz J., 2017. The impact of thermal inversion on the variability of PM10 concentration in winter seasons in Tricity. *Environment Protection Engineering*, 442: 157-172. https\\doi: 10.5277/epe170213

Daly C., Conklin D. R., Unsworth M. H., 2010. Local atmospheric decoupling in complex topography alters climate change impacts. *Int. J. Clim.*, 30(22): 1857-1864; https//doi: 10.1002/joc.2007

Dorninger M., Whiteman C. D., Bica B., Eisenbach S., Pospichal B., Steinacker R., 2011. Meteorological events affecting cold-air pools in a small basin. *Journal Appl. Meteorol. Climatol.*, 50: 2223-2234.

Dodson J. Marks D., 1997. Daily air temperature interpolated at high spatial resolution over a large mountainous region. *Clim. Res.*, 8: 1-20, https://doi.org/10.3354/cr008001.

El Melki T., 2007. Inversions thermiques et concentrations de polluants atmosphériques dans la basse troposphère de Tunis (Temperature inversions and atmospheric pollution concentrations in the low troposphere of Tunis). *Climatologie*, 4: 105-129. https://doi.org/10.4267/climatologie.773

Erpicum M., 2004. Discrimination des effets radiatifs et des effets advectifs à partir des observations de températures du réseau météo-routier de Wallonie. *Norois [on line]*, 191(2). https://doi: 10.4000/norois.1184

Fallot J.-M., 2012. *Influence de la topographie et des accumulations d'air froid sur les températures moyennes mensuelles et annuelles en Suisse*. In Bigot S. et Rome S. (eds.), 25ème colloque de l'Association Internationale de Climatologie (AIC): 273-278

Fernando H. J. S., Verhoef B., Di Sabatino S., Leo L. S., Park S., 2013. The Phoenix Evening Transition Flow Experiment TRANSFLEX. *Boundary-Layer Meteorology*, 147: 443-468. https://doi.org/10.1007/s10546-012-9795-5

Fritz B. K., Hoffman W. C., Lan Y., Thomson S. J., Huang Y., 2008. Low-level atmospheric temperature inversions and atmospheric stability: Characteristics and impacts on agricultural applications. *Atmos. Environ.*, 10: 105-130. https://doi.org/10.1016/j.atmosenv.2015.01.052.

Gardner A. S., Sharp M. J., Koerner R. M., Labine C., Boon S., Marshall S. J., Burgess D. O., Lewis D., 2009. Near-surface temperature lapse rates over Arctic glaciers and their implications for temperature downscaling. *Journal of Climate*, 2216: 4281-4298. doi:10.1175/2009JCLI2845.1

Helmis C. G., Papadopoulos K. H., 1996. Some aspects of the variation with time of katabatic flows over a simple slope. *Quarterly Journal of the Royal Meteorological Society*, 122: 595-610. https://doi.org/10.1002/qj.49712253103

Joly D., Berger A., Buoncristiani J.-F., Champagne O., Pergaud J., Richard Y., Soare P., Pohl B., 2018. Geomatic downscaling of temperatures in the Mont-Blanc massif. *Int. J. Climatol.*, 384: 1846-1863. doi:10.1002/joc.5300

Joly D., Brossard T., Cardot H., Cavailhès J., Hilal M., Wavresky P., 2010. Les types de climats en France, une construction spatiale (Types of climate in continental France, a spatial construction). *Cybergeo: European Journal of Geography*, 501. http://cybergeo.revues.org/index23155.html

Joly D., Richard Y., 2018. Topographic descriptors and thermal inversions amid the plateaus and mountains of the Jura (France). *Climatologie [Online]*, updated on: 02/10/2019. lodel.irevues.inist.fr/climatologie/index.php?id=1335.

Joly D., Richard Y., 2019. Frequency, intensity, and duration of thermal inversions in the Jura Mountains of France. *Theor. Appl. Climat.*., 1381: 639-655. https://doi.org/10.1007/s00704-019-02855-3

Kirchner M., Faus-Kessler T., Jakobi G., Leuchner M., Ries L., Scheel H. E., Suppan P., 2013. Altitudinal temperature lapse rates in an Alpine valley: trends and the influence of season and weather patterns. *Int. J. Clim.*, 333: 539-555. https//doi.org/10.1002/joc.3444

Lareau N. P., Horel J. D., 2015a. Dynamically induced displacements of a persistent cold-air pool. *Boundary-Layer Meteorology*, 154: 291-316. https://doi.org/10.1007/s10546-014-9968-5

Lareau N. P., Horel J. D., 2015b. Turbulent erosion of persistent cold-air pools: Numerical simulations. *Journal of the Atmospheric Sciences*, 724: 1409-1427. DOI: https://doi.org/10.1175/JAS-D-14-0173.1

Largeron Y., Staquet C., 2016a. The atmospheric boundary layer during wintertime persistent inversions in the Grenoble valleys. *Front. Earth Sci.*, 4(87). https//doi: 10.3389/feart.2016.00070

Largeron Y., Staquet C., 2016b. Persistent inversion dynamics and wintertime PM 10 air pollution in Alpine valleys. *Atmos. Environ.*, 135: 92-108. https//doi: 10.1016/j.atmosenv.2016.03.045

Li X., Wang L., Chen D., Yang K., Xue B., Sun L., 2013. Near-surface air temperature lapse rates in mainland China during 1962–2011. *Journal of Geophys. Research: Atmospheres*, 118(14): 7505-7515. http://doi. org/10.1002/jgrd.50553

Li Y., Yan J., Sui X., 2012. Tropospheric temperature inversion over central China. *Atmospheric Research*, 116: 105-115.

Lundquist J. D., Pepin N., Rochford C., 2008. Automated algorithm for mapping regions of cold-air pooling in complex terrain. *Journal Geophysical Research*, 113: D22107.

Mahrt L., Richardson S., Seaman N., Stauffer D., 2010. Non-stationary drainage flows and motions in the cold pool. *Tellus*, 62: 698-705. https//doi.org/10.1111/j.1600-0870.2010.00473.x

Mountain Research Initiative EDW Working Group, 2015. Elevation-dependent warming in mountain regions of the world. *Nature Clim. Change*, 5: 424-430. https://doi.org/10.1038/nclimate2563

Nigrelli G., Fratianni S., Zampollo A., Turconi L., Chiarle M., 2017. The altitudinal temperature lapse rates applied to high elevation rockfalls studies in the Western European Alps. *Theor Applied Climatol.*, 131: 1479-1491. doi: 10.1007/s00704-017-2066-0

Paraschiv V., 2010. Conditions and causes in the evolution of agriculture in the Georgeu depression. *GEOREVIEW: Scientific Annals of Stefan cel Mare University of Suceava, Geography Series*, 19(1): 143-152.

Pepin N., Norris J. R., 2005. An examination of the differences between surface and free-air temperature trend at high-elevation sites: Relationships with cloud cover, snow cover, and wind. *Journal Geophys. Res.*, 110. D24112. https://doi.org/10.1029/2005JD006150.

Pepin N., Seidel D. J., 2005. A global comparison of surface and free-air temperatures at high elevations. *J. Geophys. Res.*, 110(3): 1-15. https://doi.org/10.1029/2004JD005047.

Rolland C., 2003. Spatial and seasonal variations of air temperature lapse rates in alpine regions. *J. Climate*, 16: 1032-1046. https://doi.org/10.1175/1520-0442.

Rome S., Giorgetti J.-P., 2007. La montagne corse et ses caractéristiques climatiques. *La Météorologie*, 859: 51-52. DOI: 10.4267/2042/14846

Rupp D. E., Shafer S. L., Daly C., Jones J. A., Frey S. J. K., 2020. Temperature gradients and inversions in a forested Cascade Range basin: Synoptic- to local-scale controls. *Journal of Geophysical Research Atmospheres*, 125. e2020JD032686. https://doi.org/10.1029/2020JD032686

Schlaghamersky J., Devetter M., Hanel L., Tajovsky K., Stary J., Tuf H., Pizl V., 2014. Soil fauna across Central European sandstone ravines with temperature inversion: From cool and shady to dry and hot places. Selected papers from XVI International Colloquium on Soil Zoology & XIII International Colloquium on Apterygota, Coimbra, 2012. *Applied Soil Ecology*, 83: 30-38.

Sheridan F., Vosper S.B., Brown A. R., 2014. Characteristics of cold pools observed in narrow valleys and dependence on external conditions. *Quarterly Journal of the Royal Meteorological Society*, 140: 715-728. https://doi.org/10.1002/qj.2159

Sheridan P. F., 2019. Synoptic-flow interaction with valley cold-air pools and effects on cold-air pool persistence: Influence of valley size and atmospheric stability. *Quarterly Journal of the Royal Meteorological Society*, 145: 1636-1659. https://doi.org/10.1002/qj.3517

Vitasse Y., Klein G., Kirchner J.W., Rebetez M., 2017. Intensity, frequency, and spatial configuration of winter temperature inversions in the closed La Brévine valley, Switzerland. *Theor. Appl. Climatol.*, 130: 1073-1083. https://doi.org/10.1007/s00704-016-1944-1.

Vosper S. B., Brown A. R., 2008. Numerical simulations of sheltering in valleys: The formation of night-time cold-air pools. *Boundary-Layer Meteorology*, 127: 429-448. https://doi.org/10.1007/s10546-008-9272-3

Vosper S. B., Hughes J. K., Lock A. P., Sheridan P. F., Ross A. N., Jemmett-Smith B. C., Brown A. R., 2014. Cold pool formation in a narrow valley. *Quarterly Journal of the Royal Meteorological Society*, 140: 699-714. https://doi.org/10.1002/qj.2160

Wang S. Y., Hipps L. E., Chung O. Y., Gillies R. R., Martin R., 2015. Long-term winter inversion properties in a mountain valley of the Western United States and implications on air quality. *Journal of Applied Meteorology and Climatology*, 5412. https//doi.org/10.1175/JAMC-D-15-0172.1.

Williams R., Thorp T., 2015. Characteristics of springtime nocturnal temperature inversions in a high latitude environment. *Weather*, 70: 37-43. https://doi.org/10.1002/wea.2554

Citation of article : Joly D. et Richard Y., 2022. Temperature inversions in France – Part A: time variations. *Climatologie*, 19, 4.